Supporting Information

Korzhnev et al. 10.1073/pnas.1201799109

SI Materials and Methods

Data Analysis. As described in the main text, ^{15}N longitudinal magnetization exchange datasets (1, 2) were recorded to extract rate constants k_{MD} and k_{DM} for the exchange reaction,

$$f_M \underset{k_{DM}}{\overset{k_{MD}}{\rightleftarrows}} f_D, \tag{S1}$$

where f_M and f_D are the fractional populations of states M and D, respectively. The mixing time dependencies of auto- and cross-peak volumes were least-squares fit to the following equations:

$$
\begin{aligned}
I_{MM}(T) &= I_{MM}(0)A_M(-(\lambda_2 - a_{11})e^{-\lambda_1 T} \\
&\quad + (\lambda_1 - a_{11})e^{-\lambda_2 T})/(\lambda_1 - \lambda_2), \\
I_{DD}(T) &= I_{DD}(0)A_D(-(\lambda_2 - a_{22})e^{-\lambda_1 T} \\
&\quad + (\lambda_1 - a_{22})e^{-\lambda_2 T})/(\lambda_1 - \lambda_2), \\
I_{MD}(T) &= I_{MM}(0)A_D(a_{21}e^{-\lambda_1 T} - a_{21}e^{-\lambda_2 T})/(\lambda_1 - \lambda_2), \\
I_{DM}(T) &= I_{DD}(0)A_M(a_{12}e^{-\lambda_1 T} - a_{12}e^{-\lambda_2 T})/(\lambda_1 - \lambda_2),
\end{aligned}
\tag{S2}
$$

where $\lambda_{1,2} = \frac{1}{2}\{(a_{11} + a_{22}) \pm [(a_{11} - a_{22})^2 + 4k_{MD}k_{DM}]^{1/2}\}$; $a_{11} = R_{1M} + k_{MD}$; $a_{12} = -k_{DM}$; $a_{22} = R_{1D} + k_{DM}$; and $a_{21} = -k_{MD}$. In Eq. **S2**, R_{1M} and R_{1D} are intrinsic ^{15}N longitudinal relaxation rates for nuclei in states M and D, respectively; $I_{MM}(0)$ and $I_{DD}(0)$ denote magnetization from states M and D at the start of the mixing period, T; and A_M and A_D are factors accounting for magnetization losses during the reverse ^{15}N $\to$ ^{1}H^N transfer, calculated as described in Tollinger et al. (2).

Analysis of the magnetization exchange data described above provides a direct route for obtaining intrinsic longitudinal relaxation rates. However, a complete set of decay curves $[I_{ij}(T), \mathrm{i}, \mathrm{j} \in \{M, D\}]$ required for the analysis could be obtained for only a small number of residues (Glu15, Ala17, Phe21, Ala34, and Ser35) due to problems with peak overlap. We therefore turned to a different approach for obtaining intrinsic R_1 and R_2 relaxation rates. As described elsewhere (3, 4), ^{15}N relaxation data (R_1 and $R_{1\rho}$) were recorded where the relaxation elements (^{15}N longitudinal relaxation time, ^{15}N spin-lock) precede the t_1

period. In this case, peak intensities from states M and D are given by the sums $I_{MM}(T) + I_{DM}(T)$ and $I_{DD}(T) + I_{MD}(T)$, respectively (Eq. **S2**), and the decay is biexponential. In the analysis that we perform, intensities are fit to single exponential decay functions, leading to the extraction of effective rate constants, R_i^* (see below). The goal is to derive expressions relating these effective rates to the intrinsic rates that define the relaxation of each of the states so that the latter can be calculated. This can be achieved by approximating $I_{MM}(T) + I_{DM}(T)$ and $I_{DD}(T) + I_{MD}(T)$ by functions $I_M(T)$ and $I_D(T)$, which decay as single exponentials (as is done in the fits). We require, therefore, that

$$I_{ii}(0) + I_{ji}(0) = I_i(0) \qquad \text{and} \tag{S3}$$

$$\int_0^\infty (I_{ii}(T) + I_{ji}(T))dT = \int_0^\infty I_i(T)dT, \tag{S4}$$

where $I_i(T) = C_i \exp(-R_i^* T)$ and I_{ii}, I_{ji} are given by Eq. **S2**. From Eq. **S3** it follows that $C_M = \frac{k_{DM}}{k_{DM} + k_{MD}}$, $C_D = \frac{k_{MD}}{k_{DM} + k_{MD}}$. From Eq. **S4** we obtain (after some algebra)

$$
\begin{aligned}
R_{1M}^* &= \lambda_1 \lambda_2 / (-a_{11} - a_{21} + \lambda_1 + \lambda_2), \\
R_{1D}^* &= \lambda_1 \lambda_2 / (-a_{22} - a_{12} + \lambda_1 + \lambda_2),
\end{aligned}
\tag{S5}
$$

relating R_i^* to the intrinsic rates. Without loss in generality, values of A_M and A_D have been set to 1 in the derivation. Identical expressions hold also for transverse relaxation with $R_{1\rho,i}^*$ ($R_{1\rho,i}$) replaced by $R_{1\rho,i}^*$ ($R_{1\rho,i}$) or R_{2i}^* (R_{2i}). Intrinsic ^{15}N R_1 and $R_{1\rho}$ rates (Fig. 2C, solid lines) were calculated from the measured apparent ^{15}N relaxation rates obtained from single exponential fits of the relaxation curves R_{1i}^*, $R_{1\rho,i}^*$ (Fig. 2C, circles) by solving the system of equations, Eq. **S5**, using k_{MD} and k_{DM} values determined from analysis of magnetization exchange data. Transverse relaxation rates R_2 were calculated from R_1 and $R_{1\rho}$ as described in *Materials and Methods*.

1. Farrow NA, Zhang OW, Forman-Kay JD, Kay LE (1994) A heteronuclear correlation experiment for simultaneous determination of ^{15}N longitudinal decay and chemical-exchange rates of systems in slow equilibrium. *J Biomol NMR* 4:727–734.
2. Tollinger M, Skrynnikov NR, Mulder FAA, Forman-Kay JD, Kay LE (2001) Slow dynamics in folded and unfolded states of an SH3 domain. *J Am Chem Soc* 123:11341–11352.
3. Farrow NA, et al. (1994) Backbone dynamics of a free and a phosphopeptide-complexed Src homology-2 domain studied by ^{15}N NMR relaxation. *Biochemistry* 33:5984–6003.
4. Korzhnev DM, Skrynnikov NR, Millet O, Torchia DA, Kay LE (2002) An NMR experiment for the accurate measurement of heteronuclear spin-lock relaxation rates. *J Am Chem Soc* 124:10743–10753.
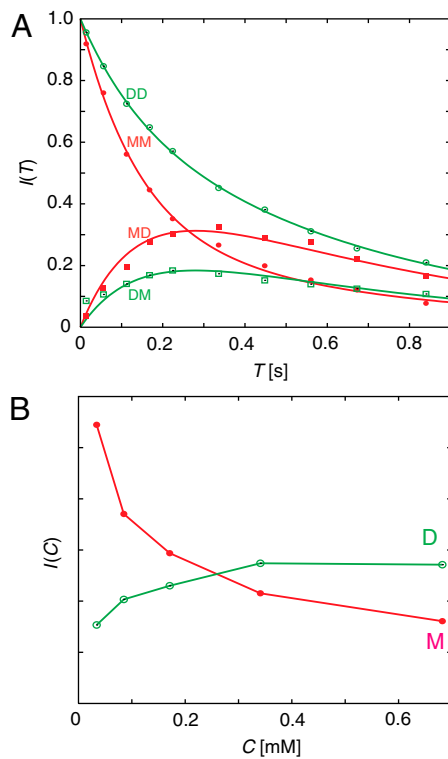
Fig. S1. (*A*) Mixing time, *T*, dependencies of autopeak (circles) and exchange cross-peak (boxes) volumes for Ser35 from magnetization exchange experiments (1, 2). The solid lines are generated from a least-squares fit of the exchange data for Ser 35 to Eq. **S2**, resulting in $k_{MD} = 3.46 \pm 0.16\ \text{s}^{-1}$ and $k_{DM} = 2.33 \pm 0.12\ \text{s}^{-1}$. (*B*) Cross-peak volumes for Ser35 measured from $^1\text{H}^\text{N}\text{-}^{15}\text{N}$ HSQC spectra of FF_{1-60} recorded as a function of protein concentration. The volumes are normalized by total protein concentration.